Scientific Report

SOURCE DATA | TRANSPARENT PROCESS

EMBO reports

RNA-processing proteins regulate Mec1/ATR activation by promoting generation of RPA-coated ssDNA

Nicola Manfrini[1], Camilla Trovesi[1], Maxime Wery[2], Marina Martina[1], Daniele Cesena[1], Marc Descrimes[2], Antonin Morillon[2,*], Fabrizio d'Adda di Fagagna[3,4,**] & Maria Pia Longhese[1,***]

Abstract

Eukaryotic cells respond to DNA double-strand breaks (DSBs) by activating a checkpoint that depends on the protein kinases Tel1/ATM and Mec1/ATR. Mec1/ATR is activated by RPA-coated single-stranded DNA (ssDNA), which arises upon nucleolytic degradation (resection) of the DSB. Emerging evidences indicate that RNA-processing factors play critical, yet poorly understood, roles in genomic stability. Here, we provide evidence that the *Saccharomyces cerevisiae* RNA decay factors Xrn1, Rrp6 and Trf4 regulate Mec1/ATR activation by promoting generation of RPA-coated ssDNA. The lack of Xrn1 inhibits ssDNA generation at the DSB by preventing the loading of the MRX complex. By contrast, DSB resection is not affected in the absence of Rrp6 or Trf4, but their lack impairs the recruitment of RPA, and therefore of Mec1, to the DSB. Rrp6 and Trf4 inactivation affects neither Rad51/Rad52 association nor DSB repair by homologous recombination (HR), suggesting that full Mec1 activation requires higher amount of RPA-coated ssDNA than HR-mediated repair. Noteworthy, deep transcriptome analyses do not identify common misregulated gene expression that could explain the observed phenotypes. Our results provide a novel link between RNA processing and genome stability.

Keywords DNA damage checkpoint; DNA double-strand breaks; Rrp6; Trf4; Xrn1
Subject Categories DNA Replication, Repair & Recombination; RNA Biology
DOI 10.15252/embr.201439458 | Received 18 August 2014 | Revised 21 November 2014 | Accepted 24 November 2014 | Published online 19 December 2014
EMBO Reports (2015) 16: 221–231

Introduction

DNA double-strand breaks (DSBs) undergo 5′–3′ nucleolytic degradation (resection) of their 5′-ending strands, to generate 3′-ended ssDNA overhangs, which are bound by the RPA complex [1]. RPA-coated ssDNA enables the checkpoint kinase Mec1/ATR to recognize DSBs [2] and facilitates the formation of continuous Rad51 filaments that initiate homologous recombination (HR) [3]. DSB resection is initiated by the MRX (Mre11-Rad50-Xrs2)/MRN (Mre11-Rad50-Nbs1) complex that acts in concert with Sae2/CtIP [4–6]. Subsequent long-range resection of the 5′ strand can occur by one of two pathways that depend on either the 5′–3′ exonuclease Exo1/hEXO1 or the Sgs1/BLM helicase in conjunction with the nuclease Dna2/hDNA2 [5,6].

Recent data indicate that RNA-processing proteins contribute to maintain genome stability either by controlling the turnover of specific transcripts or preventing accumulation of harmful DNA:RNA hybrids [7]. RNA processing can be directly involved in the DNA damage response (DDR), as some endoribonucleases have been implicated in the formation around the DSB of small non-coding RNAs that control DDR activation in both mammals and *Arabidopsis* [8,9]. Furthermore, in mammals, the endoribonuclease Ago2 facilitates the recruitment of the recombination protein Rad51 to the DSB ends [10], while the exosome recruits the activation-induced cytidine deaminase (AID) to ssDNA regions generated at divergently transcribed loci in B cells [11].

In *Saccharomyces cerevisiae*, RNA processing relies on a 5′–3′ exoribonuclease activity that is due to the Xrn protein family, which comprises one cytoplasmic (Xrn1) and one nuclear enzyme (Rat1) [12]. The nuclear exosome, whose activity is modulated by a set of cofactors including the poly(A) polymerase Trf4, is responsible for the 3′–5′ RNA-processing activity, which depends on the exoribonuclease Rrp6 [13]. Xrn1, Rrp6 and Trf4 have been shown to prevent DNA:RNA hybrid-mediated genome instability and transcription-associated hyperrecombination [14–16]. Furthermore, the lack of Trf4 leads to sensitivity to camptothecin [17], while *XRN1* deletion impairs meiotic recombination [18]. However, the precise DNA maintenance mechanisms involving these RNA decay factors remain poorly characterized. Here, we show that Xrn1, Rrp6 and

1 Dipartimento di Biotecnologie e Bioscienze, Università di Milano-Bicocca, Milan, Italy
2 Institut Curie, CNRS UMR3244, Université Pierre et Marie Curie, Paris Cedex 05, France
3 IFOM Foundation-FIRC Institute of Molecular Oncology Foundation, Milan, Italy
4 Istituto di Genetica Molecolare, Consiglio Nazionale delle Ricerche, Pavia, Italy
*Corresponding author. Tel: +33 156246570; Fax: +33 156246674; E-mail: antonin.morillon@curie.fr
**Corresponding author. Tel: +39 02574303227; Fax: +39 02574303231; E-mail: fabrizio.dadda@ifom.eu
***Corresponding author. Tel: +39 0264483425; Fax: +39 0264483565; E-mail: mariapia.longhese@unimib.it

Trf4 participate in the activation of the checkpoint kinase Mec1 by promoting the formation of RPA-coated ssDNA at DSB ends. These findings reveal a novel role for RNA decay factors in the maintenance of genome integrity.

Results and Discussion

Xrn1, Rrp6 and Trf4 are necessary for Mec1/ATR activation in response to a DSB

To investigate the role of Xrn1, Rrp6 and Trf4 in the DDR, yeast strains carrying the deletion of the corresponding genes were tested for sensitivity to DNA damaging agents. The *xrn1*Δ, *rrp6*Δ and *trf4*Δ mutants were hypersensitive to the DSB-inducing agent phleomycin, with *xrn1*Δ cells showing the strongest sensitivity (Fig 1A), suggesting that the corresponding proteins are involved, directly or indirectly, in the cellular response to DSBs.

Next, we asked whether *xrn1*Δ, *rrp6*Δ and *trf4*Δ cells were defective in checkpoint activation in response to a single DSB. To address this question, we deleted *XRN1*, *RRP6* or *TRF4* in a haploid strain carrying the *HO* gene under the control of a galactose-inducible promoter. In this strain, induction of HO by galactose addition leads to the generation at the *MAT* locus of a single DSB that cannot be repaired by HR due to the lack of the homologous donor loci *HML* and *HMR* [19]. *HO* expression was induced by transferring to galactose wild-type, *xrn1*Δ, *rrp6*Δ and *trf4*Δ cells exponentially growing in raffinose. Checkpoint activation was monitored by following Rad53 phosphorylation, which is required for Rad53 activation and is detectable as a decrease of its electrophoretic mobility. As shown in Fig 1B, the amount of phosphorylated Rad53 after HO induction was much lower in *xrn1*Δ, *rrp6*Δ and *trf4*Δ than in wild-type cells. Furthermore, when the same strains were arrested in G1 with α-factor and then spotted on galactose-containing plates to induce HO, *xrn1*Δ, *rrp6*Δ and *trf4*Δ cells formed microcolonies with more than 2 cells more efficiently than similarly treated wild-type cells (Fig 1C), indicating a defect in DSB-induced cell cycle arrest. Although *xrn1*Δ, *rrp6*Δ and *trf4*Δ cells slightly delayed the G1/S transition under unperturbed conditions (Fig 1D), their checkpoint defect was not due to altered cell cycle progression, as *xrn1*Δ, *rrp6*Δ and *trf4*Δ were defective in Rad53 phosphorylation also when the HO cut was induced in G2-arrested cells that were kept arrested in G2 throughout the experiment (Fig 1E).

The requirement of Xrn1, Rrp6 and Trf4 for DSB-induced checkpoint activation was not locus specific, as *xrn1*Δ, *rrp6*Δ and *trf4*Δ cells were defective in Rad53 phosphorylation also when the HO-induced DSB was generated at the *LEU2* locus (Fig 1F). Neither it was influenced by the level of transcription of the DNA region in which the DSB occurs, as the amount of Rad53 phosphorylation in wild-type, *xrn1*Δ, *rrp6*Δ and *trf4*Δ cells after HO-induced DSB formation into the *LEU2* gene was similar to that detected when the DSB was generated into the *LEU2* gene lacking its promoter (Supplementary Fig S1).

Xrn1 and Rrp6 promote checkpoint activation by acting as exoribonucleases. In fact, cells carrying the *xrn1-E176G* or the *rrp6-D238A* allele, encoding nuclease-defective Xrn1 [20] or Rrp6 [21] variants, were as defective in HO-induced Rad53 phosphorylation as *xrn1*Δ and *rrp6*Δ cells, respectively (Fig 1G).

In *S. cerevisiae*, checkpoint activation in response to a single DSB is completely dependent on Mec1 [22], suggesting that *xrn1*Δ, *rrp6*Δ and *trf4*Δ cells might be defective in Mec1 activation. Indeed, *xrn1*Δ, *rrp6*Δ and *trf4*Δ cells were defective in phosphorylation of the Mec1 specific target Ddc2 after HO induction (Fig 1H), indicating that the lack of Xrn1, Rrp6 or Trf4 impairs Mec1 signaling activity.

Xrn1 promotes resection of DNA ends

While Xrn1 controls cytoplasmic RNA decay, RNA processing into the nucleus depends on its nuclear paralog Rat1 [23]. Targeting Rat1 into the cytoplasm by deleting its nuclear localization sequence (*rat1-ΔNLS*) restores Xrn1-like function in mRNA degradation [23], prompting us to test whether it could restore Rad53 phosphorylation after DSB formation in *xrn1*Δ cells. Strikingly, expression of the *rat1-ΔNLS* allele on a centromeric plasmid, but not of wild-type *RAT1*, suppressed both the Rad53 phosphorylation defect (Fig 2A) and the hypersensitivity to phleomycin (Fig 2B) of *xrn1*Δ cells, indicating that Xrn1 controls checkpoint activation by acting in the cytoplasm.

Mec1 activation requires formation of RPA-coated ssDNA, which arises from 5′ to 3′ nucleolytic degradation of the DSB ends [2]. To assess whether the inability of *xrn1*Δ cells to activate Mec1/ATR

Figure 1. The lack of Xrn1, Rrp6 or Trf4 impairs Mec1 checkpoint signaling in response to a DSB.

A Sensitivity to phleomycin. Serial dilutions (1:10) of exponentially growing cell cultures were spotted out onto YEPD plates with or without phleomycin (phleo).

B Rad53 phosphorylation after a DSB at the *MAT* locus. YEPR exponentially growing cell cultures of JKM139 derivative strains, carrying the HO cut site at the *MAT* locus, were transferred to YEPRG at time zero. Protein extracts from samples taken at the indicated times after HO induction were subjected to Western blot analysis with anti-Rad53 antibodies.

C Checkpoint-mediated cell cycle arrest. G1-arrested JKM139 derivative cells were plated on galactose-containing plates at time zero. Two hundred cells for each strain were analyzed to determine the frequency of cells that were unbudded, large budded or forming microcolonies with more than two cells.

D Analysis of cell cycle progression in unperturbed conditions. Cell cultures arrested in G1 with α-factor were released into YEPD at time zero. FACS analysis of DNA content.

E Checkpoint activation in G2-arrested cells. As in (B) except that HO was induced in nocodazole-arrested JKM139 derivative cells that were kept arrested in G2 in the presence of nocodazole throughout the experiment.

F Rad53 phosphorylation after a DSB at the *LEU2* locus. As in (B), but inducing HO expression in YFP17 derivative strains, which carry the HO cut site at the *LEU2* locus.

G Checkpoint activation. Protein extracts from JKM139 derivative strains containing the indicated centromeric plasmids were subjected to Western blot analysis with anti-Rad53 antibodies at different time points after HO induction.

H Ddc2 phosphorylation after a DSB at the *MAT* locus. Protein extracts from JKM139 derivative strains expressing fully functional Ddc2-HA were subjected to Western blot analysis with anti-HA antibodies at different time points after HO induction.

Source data are available online for this figure.

could be related to defects in DSB resection, we directly monitored ssDNA generation at the DSB ends. Cells exponentially growing in raffinose were transferred to galactose to induce HO and genomic DNA was analyzed at different time points after HO induction. Because ssDNA is resistant to cleavage by restriction enzymes, 5′ strand resection can be measured by following the loss of SspI restriction fragments by Southern blot analysis under alkaline conditions using a ssRNA probe that anneals to the unresected strand on

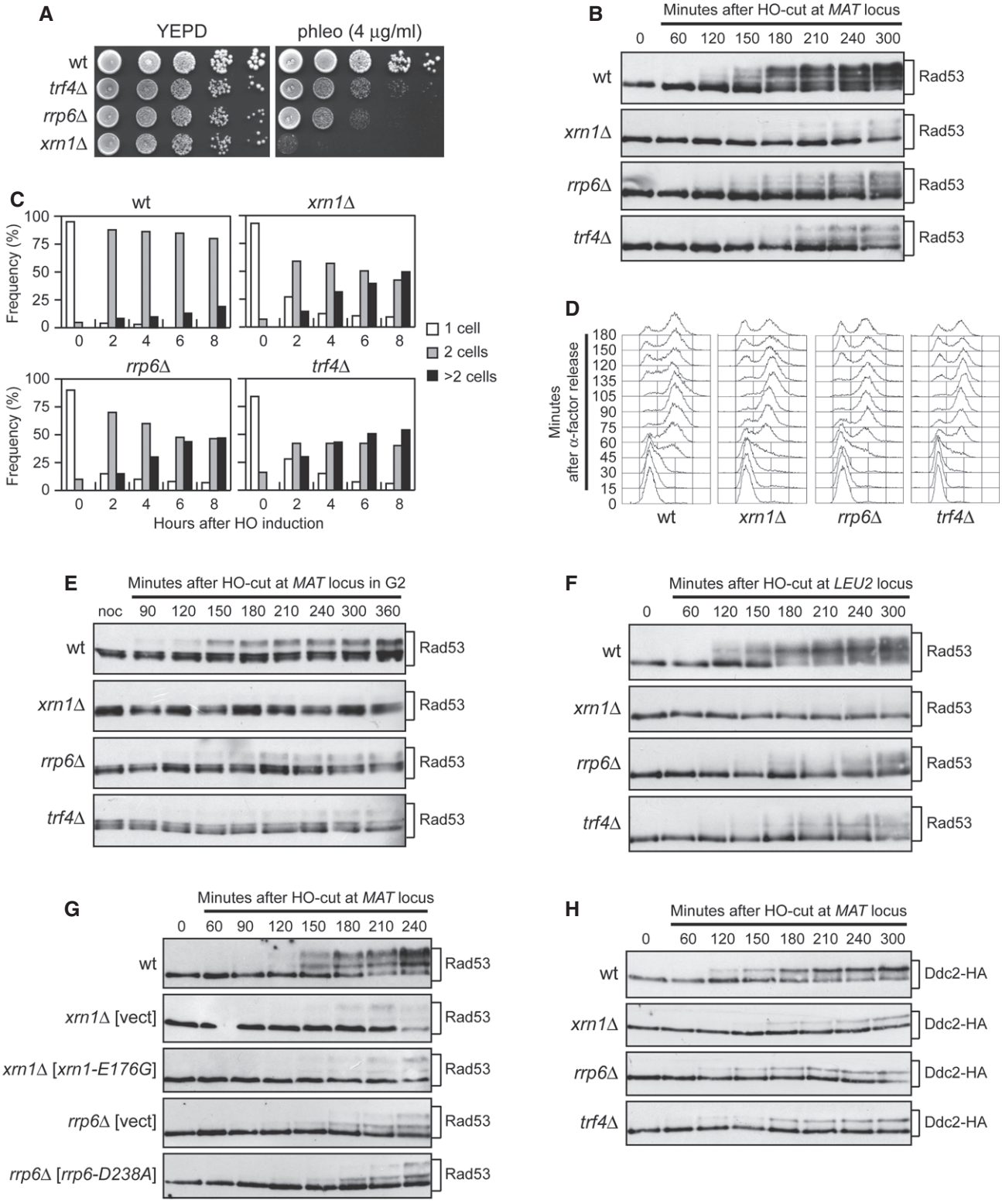

Figure 1.

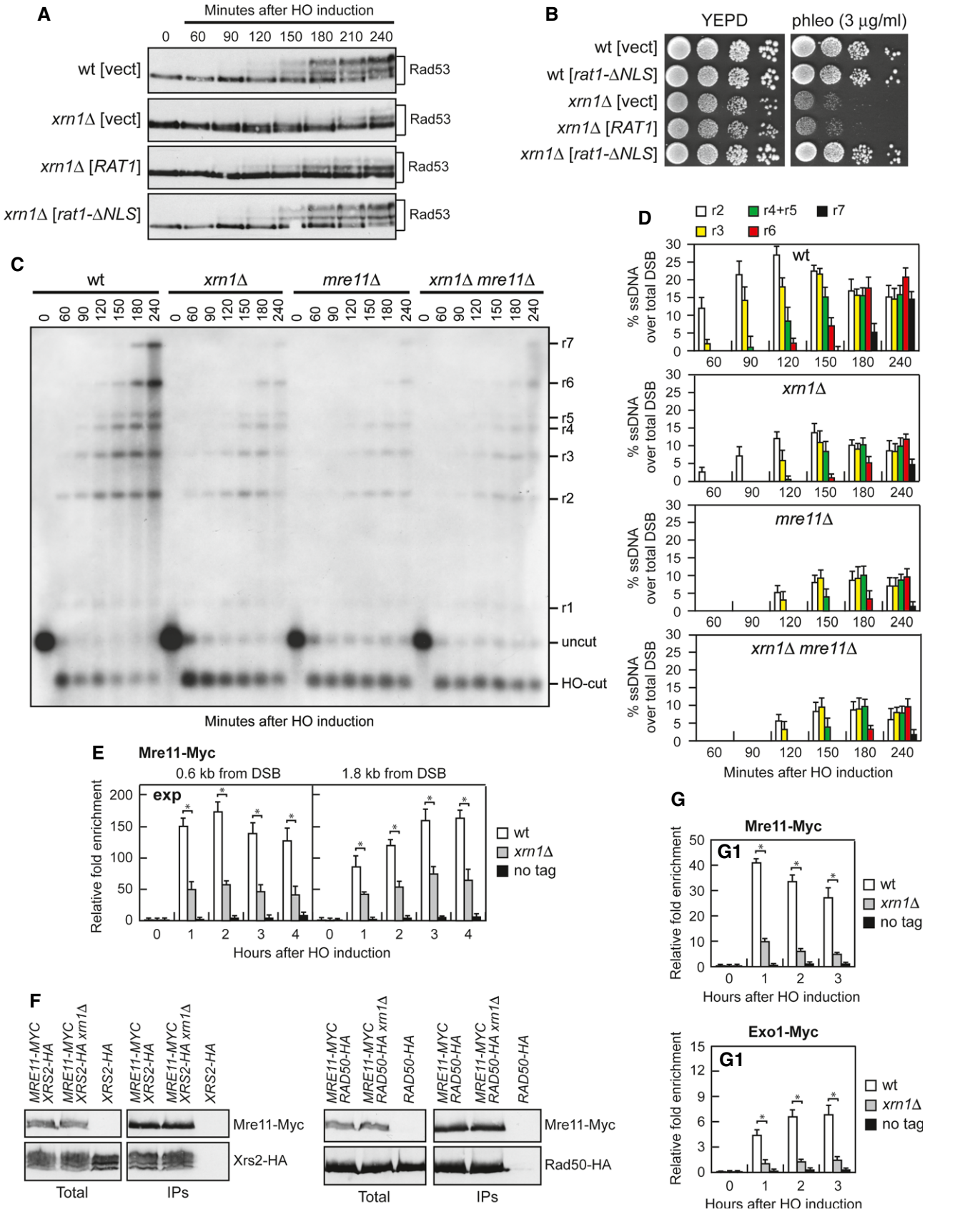

Figure 2.

Figure 2. The lack of Xrn1 impairs DSB resection and Mre11 recruitment to the DSB.

A Checkpoint activation. Protein extracts from JKM139 derivative strains containing the indicated centromeric plasmids were subjected to Western blot analysis with anti-Rad53 antibodies at different time points after HO induction.

B Sensitivity to phleomycin. Strains in (A) were serially diluted (1:10) and spotted out onto YEPD plates with or without phleomycin.

C DSB resection. YEPR exponentially growing cultures of JKM139 derivative cells were transferred to YEPRG at time zero. Gel blots of SspI-digested genomic DNA separated on alkaline agarose gel were hybridized with a single-stranded RNA probe that anneals to the unresected strand on one side of the break. 5′–3′ resection progressively eliminates SspI sites (S), producing larger SspI fragments (r1 through r7) detected by the probe.

D Densitometric analyses. The experiment as in (C) was independently repeated three times and the mean values are represented with error bars denoting SD ($n = 3$).

E Mre11-Myc recruitment at the HO-induced DSB. In all diagrams, data are expressed as fold enrichment at the HO-induced DSB over that at the non-cleaved *ARO1* locus, after normalization of ChIP signals to the corresponding input for each time point. The mean values are represented with error bars denoting SD ($n = 3$). $^*P < 0.01$, *t*-test.

F MRX complex formation. Protein extracts were analyzed by Western blot with anti-Myc or anti-HA antibodies either directly (Total) or after Mre11-Myc immunoprecipitation (IPs) with anti-Myc antibodies.

G Mre11 recruitment at the HO-induced DSB in G1-arrested *xrn1*Δ cells. ChIP analysis was performed as in (E) except that HO was induced in α-factor-arrested JKM139 derivative cells kept arrested in G1 with α-factor throughout the experiment. qPCR was performed at 1.8 kb from the DSB. The mean values are represented with error bars denoting SD ($n = 3$). $^*P < 0.01$, *t*-test.

Source data are available online for this figure.

one side of the break. The appearance of ssDNA intermediates was delayed in galactose-induced *xrn1*Δ cells compared to wild-type (Fig 2C and D), indicating that the lack of Xrn1 impairs generation of ssDNA at the DSB ends.

DSB resection is under the control of several proteins, which act as positive (Mre11, Rad50, Xrs2, Dna2, Sgs1 and Exo1) or negative (Rad9) regulators [1]. The resection defect of *xrn1*Δ was not due to lower amounts of the above proteins, as similar amounts of Mre11, Rad50, Xrs2, Sgs1, Exo1 and Rad9 proteins could be detected in both wild-type and *xrn1*Δ cells (Supplementary Fig S2). The amount of Dna2 was higher in *xrn1*Δ than in wild-type cells (Supplementary Fig S2), but this effect did not account by itself for the DSB resection defect of *xrn1*Δ cells, as *DNA2* overexpression did not affect either checkpoint activation or generation of ssDNA at the DSB ends in wild-type cells (data not shown).

Xrn1 supports MRX function in DSB resection

As the lack of Xrn1 impairs initiation of DSB processing, which is known to require the MRX complex, we investigated whether it might affect MRX function. Epistasis analysis revealed that DSB resection in the *xrn1*Δ *mre11*Δ double mutant was as defective as in the *mre11*Δ single mutant (Fig 2C and D), indicating that Xrn1 and MRX promote DSB resection by acting in the same pathway. Chromatin immunoprecipitation (ChIP) and quantitative real-time PCR showed that Mre11 association at the HO-induced DSB was lower in *xrn1*Δ than in wild-type cells (Fig 2E). This decreased binding was not due to lower Mre11 protein level (Supplementary Fig S2) or altered MRX complex formation (Fig 2F). Neither it was due to different resection kinetics, as the lack of Xrn1 impaired Mre11 recruitment even when the DSB was induced in G1-arrested cells (Fig 2G), where DSB resection is very poor due to low Cdk1 activity [24]. Consistent with MRX being required to load Exo1 and Dna2 at the DSB [25], Exo1 association at the HO-induced DSB was lower in *xrn1*Δ than in wild-type cells (Fig 2G), and similar results were obtained for Dna2 (data not shown). Thus, Xrn1 regulates DSB resection likely by promoting MRX recruitment to the DSB.

Rrp6 and Trf4 promote the loading of RPA and Mec1 to the DSB

Resection intermediates accumulated with wild-type kinetics in *rrp6*Δ and *trf4*Δ cells (Fig 3A and B), indicating that the defective checkpoint response in these mutants cannot be ascribed to reduced generation of ssDNA at the DSB. As Mec1 recognizes and is activated by RPA-coated ssDNA [2], the checkpoint defect of *rrp6*Δ and *trf4*Δ cells might be due to the inability of either Mec1 itself or RPA to bind ssDNA. Indeed, the lack of Rrp6 or Trf4 impaired Mec1 and Rpa1 association at the DSB (Fig 3C and D), although similar amounts of Mec1 (Fig 3E) and RPA complex (Fig 3F) can be detected in protein extracts from wild-type, *rrp6*Δ and *trf4*Δ cells. This decreased RPA recruitment to the DSB was not due to defects in either RPA complex formation (Fig 3G) or RPA sub-cellular localization (Supplementary Fig S3A). Thus, Rrp6 and Trf4 appear to regulate Mec1 activation by promoting association to the DSB ends of RPA, and therefore of Mec1.

Interestingly, Rrp6 and Trf4 promoted Mec1 activation not only in response to a HO-induced DSB, but also after treatment with methyl methane sulfonate (MMS) or hydroxyurea (HU) (Fig 3H), suggesting that they favor RPA loading also to the ssDNA generated during replicative stress.

Rrp6 and Trf4 are not required for HR repair of a DSB

After covering ssDNA, RPA is displaced by Rad51 [3]. Reduced RPA binding in *rrp6*Δ and *trf4*Δ cells was due to a less efficient RPA loading rather than to a more efficient RPA displacement by Rad51 and/or Rad52. In fact, RPA was still poorly recruited at the DSB ends in *rrp6*Δ and *trf4*Δ cells lacking either Rad51 or Rad52 (Fig 4A).

As RPA promotes localization of the recombination proteins Rad51 and Rad52 to initiate DSB repair by HR [26], the lack of Rrp6 and/or Trf4 may affect the loading of Rad51 and/or Rad52 on the DSB. This does not seem to be the case, as similar amounts of Rad51 and Rad52 were detected in wild-type, *rrp6*Δ and *trf4*Δ cells, both in total protein extracts (Fig 4B) and bound at the DSB (Fig 4C and D).

Rad51-dependent recombination leads to the formation of noncrossover or crossover products. We analyzed the formation of such recombination products using a haploid strain that bears a *MATa* sequence on chromosome V and an uncleavable *MATa-inc* sequence on chromosome III [27]. Upon galactose addition, the HO-induced DSB can be repaired using the *MATa-inc* sequence as a donor, resulting in crossover and non-crossover products (Fig 4E). Consistent with the finding that the lack of Rrp6 did not impair Rad51 and Rad52 loading at the DSB, the overall DSB repair

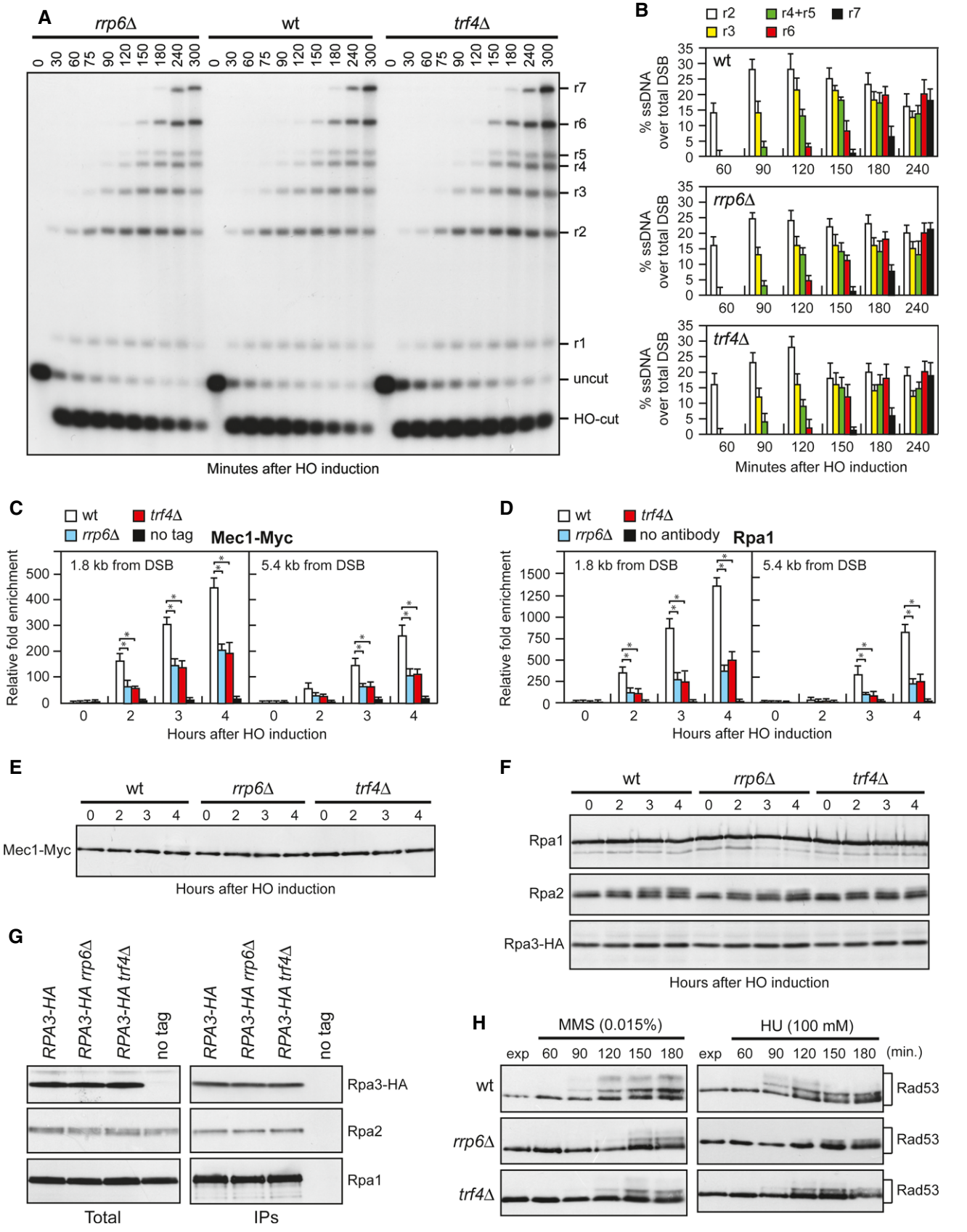

Figure 3.

Figure 3. The lack of Rrp6 or Trf4 impairs RPA and Mec1 recruitment to the DSB without affecting DSB resection.

A DSB resection. Genomic DNA was analyzed for ssDNA formation as described in Fig 2C.

B Densitometric analyses. The experiment as in (A) was independently repeated three times and the mean values are represented with error bars denoting SD ($n = 3$).

C Mec1-Myc recruitment at the HO-induced DSB. In all diagrams, data are expressed as fold enrichment at the HO-induced DSB over that at the non-cleaved *ARO1* locus, after normalization of ChIP signals to the corresponding input for each time point. The mean values are represented with error bars denoting SD ($n = 3$). *$P < 0.01$, *t*-test.

D Rpa1 recruitment at the HO-induced DSB. ChIP analysis was performed as in (C). The mean values are represented with error bars denoting SD ($n = 3$). *$P < 0.01$, *t*-test.

E Mec1 protein level. Western blot with anti-Myc antibodies of extracts used for the ChIP analysis shown in (C).

F Rpa1, Rpa2 and Rpa3 protein levels. Western blot with anti-Rpa1, anti-Rpa2 and anti-HA antibodies of extracts used for the ChIP analysis in (D).

G RPA complex formation. Protein extracts were analyzed by Western blotting with anti-HA (Rpa3), anti-Rpa1 or anti-Rpa2 antibodies either directly (Total) or after Rpa3-HA immunoprecipitation (IPs) with anti-HA antibodies.

H Checkpoint activation in response to HU and MMS treatment. Western blot analysis with anti-Rad53 antibodies of protein extracts prepared from exponentially growing cells that were treated with HU or MMS for the indicated time points.

Source data are available online for this figure.

efficiency in *rrp6*Δ cells was similar to that observed in wild-type cells (Fig 4F and G). By contrast, DSB repair efficiency was reduced in *xrn1*Δ cells (Fig 4F and G), in agreement with the finding that these cells were defective in the generation of ssDNA (Fig 2C and D) that is necessary to catalyze strand invasion and base pairing. Therefore, the lack of Rrp6 or Trf4 appears to specifically impair the loading at the DSB ends of RPA, but not of Rad51 and Rad52.

The lack of Xrn1, Rrp6 or Trf4 does not affect expression of most DDR genes

As the lack of Xrn1 or Rrp6/Trf4 might influence the recruitment of MRX or RPA, respectively, by regulating gene expression, we performed deep transcriptome analyses before and after generation of the HO-induced DSB. Biological duplicates of cells exponentially growing in raffinose (time zero) were shifted to galactose for 60 and 240 min to induce HO, and total RNA was subjected to strand-specific whole transcriptome analysis. The vast majority of protein-coding genes in a wild-type context showed no significant change of expression 60 min (Spearman's correlation coefficient 0.98; Fig 5A) and 240 min (Spearman's correlation coefficient 0.95; Fig 5B) after HO induction. Expression of genes coding for factors involved in DDR (see list in Supplementary Table S1) also remained globally unchanged (Fig 5C and D), with 0.96–0.98 and 0.89–0.94 Spearman's correlation coefficients 60 min (Fig 5A) and 240 min (Fig 5B) after HO induction, respectively. Further differential expression analysis to obtain better statistical validation revealed that only 5 of 193 DDR genes were affected (fold change ≤ 0.5 or ≥ 2, $P \leq 0.001$) 240 min after HO induction (Supplementary Fig S4A and B, see list in Supplementary Table S2), indicating that the HO-induced DSB has little impact on the transcriptome.

When we performed similar analyses in strains lacking Xrn1, Rrp6 or Trf4, as previously reported [28], we observed that inactivation of Xrn1 resulted in global stabilization of mRNAs (Fig 5C and D; Supplementary Fig S4F). In contrast, mRNA levels in *rrp6*Δ and *trf4*Δ cells were similar to wild-type (Fig 5C and D, Supplementary Fig S4G and H). Importantly, in all tested strains and conditions, DDR genes showed expression similar to all genes (Fig 5D). Deeper differential expression analysis showed that the majority of DDR mRNAs remained unchanged (Fig 5C and Supplementary Fig S4C–E), although some of them were misregulated in these mutants (3 in *rrp6*Δ, 22 in *xrn1*Δ and 27 in *trf4*Δ, Supplementary Table S2). Further studies are required to assess whether these mRNA misregulations might account for the DSB resection defect of *xrn1*Δ cells, but the finding that Xrn1 acts in the checkpoint as a cytoplasmic exoribonuclease makes them potential candidates.

The only three genes (*SMC6*, *HPA2* and *RLF2*) that are downregulated in *rrp6*Δ cells are not affected in *trf4*Δ and vice versa (Supplementary Table S2), making it unlikely that these altered mRNA levels may account for the reduced recruitment of RPA to the ssDNA ends displayed by both *rrp6*Δ and *trf4*Δ cells. In addition, while *SMC6* is essential for cell viability, deletion of *RLF2*, which encodes the largest subunit of the Chromatin Assembly Factor CAF-1, or *HPA2*, which encodes a histone acetyltransferase, did not impair checkpoint activation in response to the HO-induced DSB [29, data not shown]. Of note, the lack of Trf4 increased the amount of mRNAs encoding histones H2A, H3 and H4 (Supplementary Table S2). However, these upregulations did not cause any increase of the corresponding protein levels (Supplementary Fig S3B), consistent with previous findings that RNA decay mutants accumulate mRNA intermediates that might not be efficiently translated [12,13].

In summary, our data show that Xrn1, Rrp6 and Trf4 proteins regulate Mec1 signaling activity by promoting formation of RPA-coated ssDNA at the DSB ends, thus linking RNA processing to the checkpoint response. While Xrn1 is required to generate ssDNA by promoting MRX recruitment to the DSB, Rrp6 and Trf4 are required to recruit RPA, and therefore Mec1/ATR, to the ssDNA ends. Although the amount of RPA recruited at the DSB in *rrp6*Δ and *trf4*Δ cells appears to be below the threshold necessary for full checkpoint activation, it is enough for Rad51 and Rad52 loading to the DSB and for subsequent HR repair. This finding suggests that full Mec1 activation requires a higher amount of RPA-coated ssDNA than HR-mediated repair events, thus ensuring checkpoint activation only when the DSB cannot be rapidly repaired. How Rrp6 and Trf4 control the association of RPA with ssDNA requires further studies. One possibility is that the lack of Rrp6 or Trf4 increases the persistence around the DSB site of RNA molecules that can inhibit RPA recruitment by annealing with the ssDNA generated during DSB resection. However, overproduction of the Ribonuclease H1 Rnh1, which is known to decrease endogenous RNA:DNA hybrids *in vivo* [15], did not restore either Rad53 phosphorylation or RPA association to the DSB (Supplementary Fig S5A and B) in *rrp6*Δ and *trf4*Δ cells. As RPA binds to ssDNA in two conformational states that differ both in affinity of the bound DNA and in the length of the contacted ssDNA [30], we favor the hypothesis that Rrp6 and Trf4

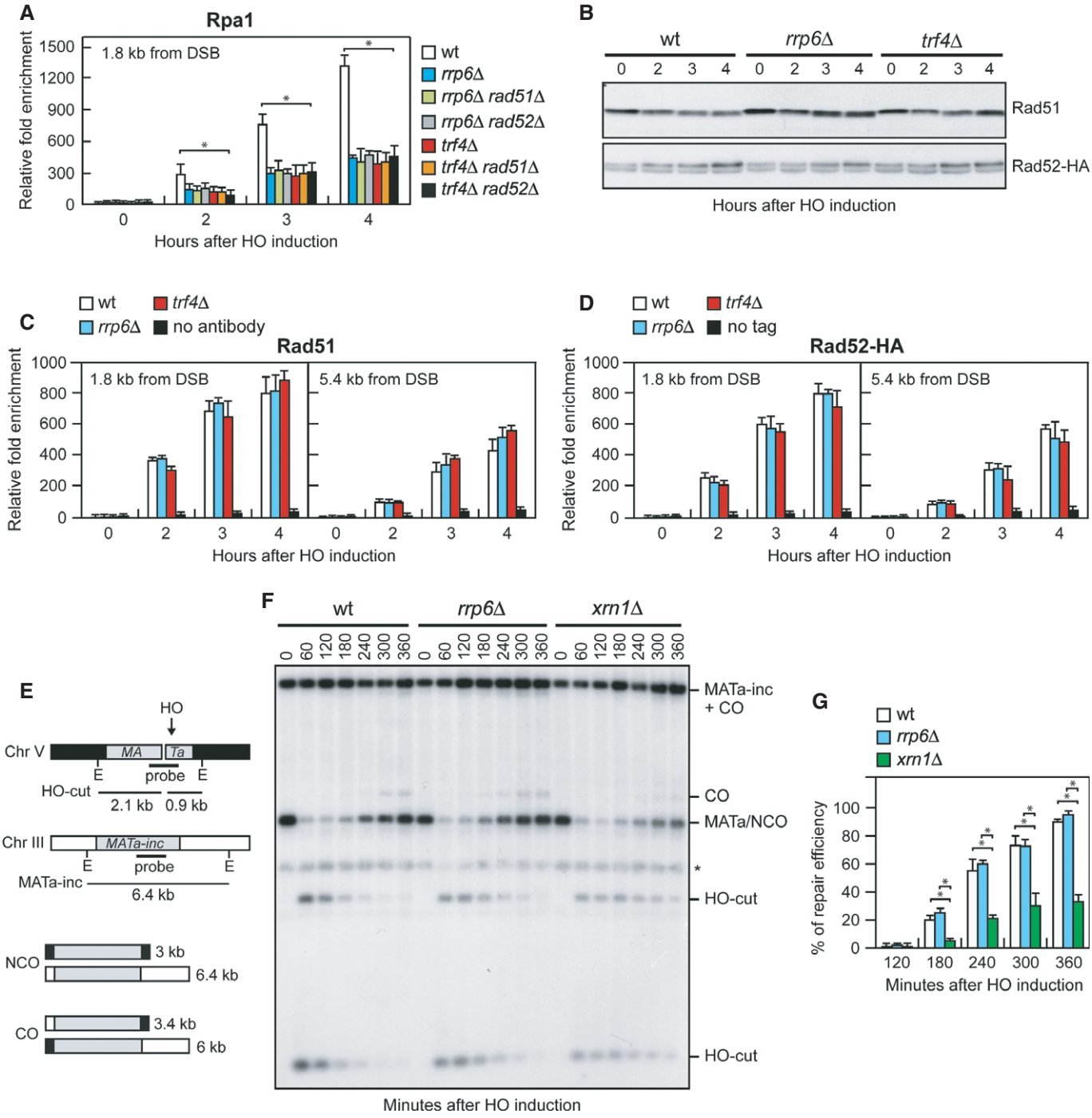

Figure 4. The lack of Rrp6 or Trf4 does not affect DSB repair by HR.

A Recruitment of Rpa1 at the HO-induced DSB. ChIP analysis was performed as in Fig 3D. The mean values are represented with error bars denoting SD (n = 3). *P < 0.01, t-test.

B Rad51 and Rad52 protein levels. Western blot with anti-Rad51 and anti-HA antibodies of extracts used for the ChIP analysis in (C) and (D), respectively.

C, D Recruitment of Rad51 and Rad52-HA at the HO-induced DSB. ChIP analysis was performed as in Fig 3. The mean values are represented with error bars denoting SD (n = 3). *P < 0.01, t-test.

E System to detect CO and NCO. Galactose-induced HO generates a DSB at the *MATa* locus on chromosome V that is repaired by using the homologous *MATa-inc* region on chromosome III. Sizes of EcoRI (E) DNA fragments detected by the probe are indicated.

F Detection of DSB repair products. EcoRI-digested genomic DNA from samples taken at the indicated times after HO induction was subjected to Southern blot analysis with the *MATa* probe depicted in (E). *indicates a cross hybridization signal.

G Densitometric analysis of the repair signals. The mean values are represented with error bars denoting SD (n = 3). *P < 0.01, t-test.

Source data are available online for this figure.

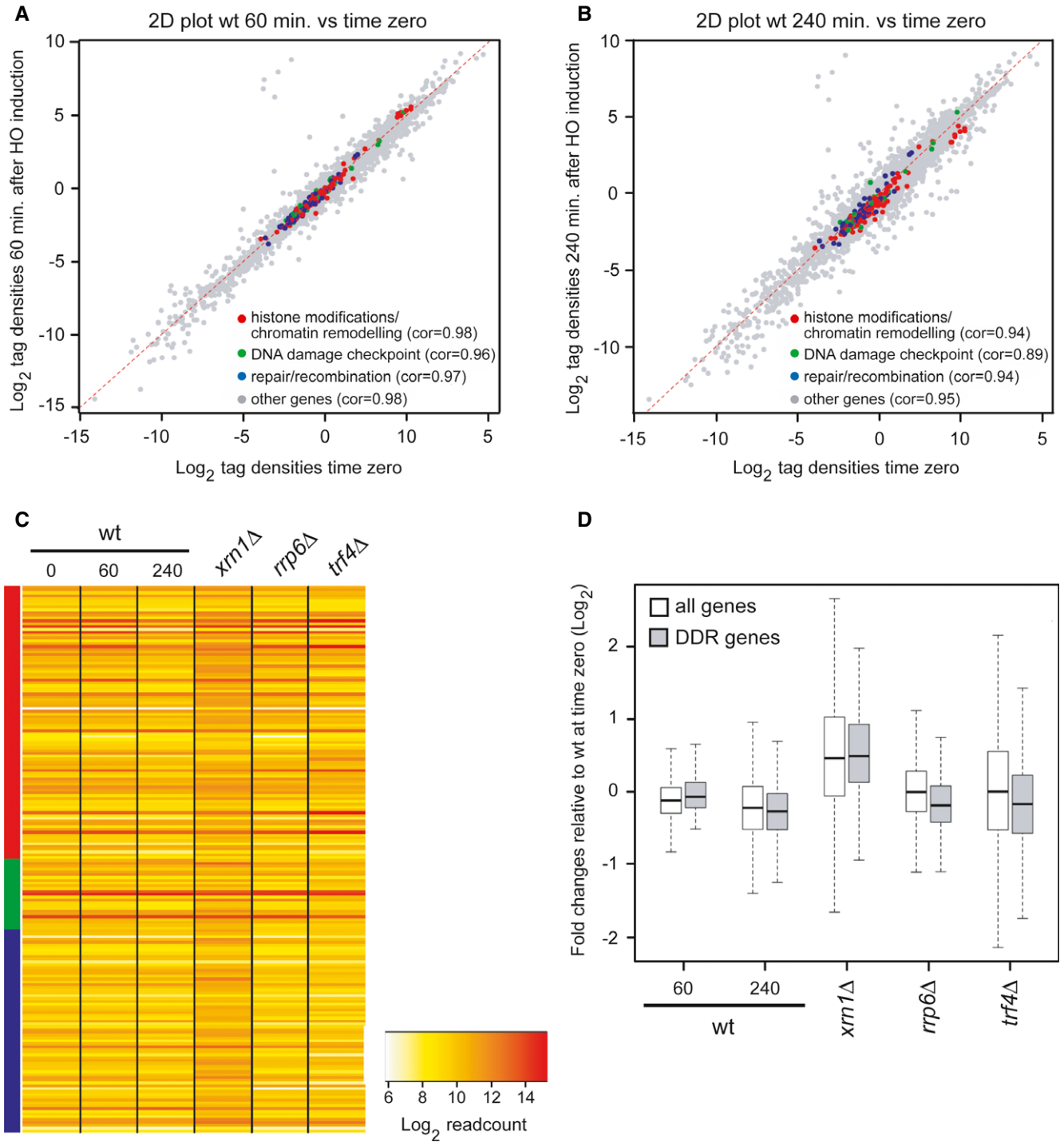

Figure 5. The lack of Xrn1, Rrp6 or Trf4 does not impair expression of most DDR genes.

A Expression of DDR genes in wild-type cells 60 min after HO induction. Scatter plot of tag density for genes encoding DDR factors in wild-type strain (JKM139) before (time zero) and after (60 min) HO induction. Results are presented as $\log_2$ of density, expressed in tag per nucleotide. Spearman's correlation coefficients for each set of genes are indicated.

B Expression of DDR genes in wild-type cells 240 min after HO induction. Same as in (A) using JKM139 cells at time zero and 240 min after HO induction.

C Expression of DDR genes in wild-type cells at time zero, 60 and 240 min after HO induction, and in *xrn1Δ*, *rrp6Δ* and *trf4Δ* cells at time zero. Data are presented as a heatmap and genes are clustered according the classification used in (A), with the same color code.

D Global expression of all protein-coding and DDR genes upon HO induction or inactivation of RNA decay factors. Box plot representation of expression fold change for all protein-coding (white) and DDR (gray) genes in wild-type cells 60 and 240 min after HO induction, and in *xrn1Δ*, *rrp6Δ* and *trf4Δ* mutants at time zero. All fold changes are relative to the wild-type at time zero. For each condition, the black line within the box corresponds to the median value, while the top and bottom lines of the box correspond to the upper quartile and lower quartile, respectively (n = 5,798 for all genes and n = 194 for the DDR genes). Outliers are not represented.

may modulate directly or indirectly these RPA conformational changes, and therefore RPA ability to bind ssDNA. As RNA-processing factors are evolutionary conserved, our findings highlight a novel important mechanism through which RNA-processing proteins can preserve genome integrity.

Materials and Methods

Yeast strains and plasmids

Strain genotypes are listed in Supplementary Table S3. Cells were grown in YEP medium (1% yeast extract, 2% bactopeptone) supplemented with 2% glucose (YEPD), 2% raffinose (YEPR) or 2% raffinose and 3% galactose (YEPRG).

DSB resection and repair

DSB end resection at the *MAT* locus in JKM139 derivative strains was analyzed on alkaline agarose gels. Quantitative analysis of DSB resection was performed by calculating the ratio of band intensities for ssDNA and total amount of DSB products.

ChIP analysis

Data are expressed as fold enrichment at the HO-induced DSB over that at the non-cleaved *ARO1* locus, after normalization of ChIP signals to the corresponding input for each time point. Fold enrichment was then normalized to the efficiency of DSB induction.

Total RNA-Seq analysis

For each yeast strain and condition, total RNA-Seq analysis was performed from two biological replicates. Sequence data are publicly available at Gene Expression Omnibus (GEO) (accession number GSE63444) and at http://vm-gb.curie.fr/dsb/.

For more detailed Materials and Methods see the Supplementary Information.

Supplementary information for this article is available online: http://embor.embopress.org

Acknowledgements

We thank A. Aguilera, J.S. Butler, J. Haber and A.W. Johnson for strains and plasmids; N. Lowndes and B. Stillman for antibodies; G. Lucchini for critical reading of the manuscript. M.P.L. is supported by Associazione Italiana per la Ricerca sul Cancro (AIRC) (grant IG15210), and PRIN 2010–2011. A.M. is supported by the ANR "REGULncRNA" and ERC "EpincRNA" starting grant. F.d'A.d.F. is supported by AIRC (grant IG12971), Human Frontier Science Program (contract number: RGP 0014/2012), Cariplo Foundation (grant number 2010.0818), FP7 PEOPLE 2012 ITN (CodAge), Telethon (GGP12059), AICR, PRIN 2010-2011, MIUR EPIGEN Project and European Research Council advanced grant (322726). High-throughput sequencing was performed by the NGS platform of Institut Curie, supported by the grants ANR-10-EQPX-03 and ANR10-INBS-09-08 from the Agence Nationale de la Recherche (investissements d'avenir) and by the Canceropôle Ile-de-France. NM and CT were supported by fellowships from Fondazione Italiana per la Ricerca sul Cancro (FIRC).

Author contributions

Fd'AdF conceived the project. NM, AM, Fd'AdF and MPL conceived and designed the experiments. NM, CT, MW, MM and DC performed the experiments. NM, CT, MW, MD, AM, Fd'AdF and MPL analyzed the data. MPL wrote the paper.

Conflict of interest

The authors declare that they have no conflict of interest.

References

1. Longhese MP, Bonetti D, Manfrini N, Clerici M (2010) Mechanisms and regulation of DNA end resection. *EMBO J* 29: 2864 – 2874
2. Zou L, Elledge SJ (2003) Sensing DNA damage through ATRIP recognition of RPA-ssDNA complexes. *Science* 300: 1542 – 1548
3. Jasin M, Rothstein R (2013) Repair of strand breaks by homologous recombination. *Cold Spring Harb Perspect Biol* 5: a012740
4. Cannavo E, Cejka P (2014) Sae2 promotes dsDNA endonuclease activity within Mre11-Rad50-Xrs2 to resect DNA breaks. *Nature* 514: 122 – 125
5. Mimitou EP, Symington LS (2008) Sae2, Exo1 and Sgs1 collaborate in DNA double-strand break processing. *Nature* 455: 770 – 774
6. Zhu Z, Chung WH, Shim EY, Lee SE, Ira G (2008) Sgs1 helicase and two nucleases Dna2 and Exo1 resect DNA double-strand break ends. *Cell* 134: 981 – 994
7. Dutertre M, Lambert S, Carreira A, Amor-Guéret M, Vagner S (2014) DNA damage: RNA-binding proteins protect from near and far. *Trends Biochem Sci* 39: 141 – 149
8. Francia S, Michelini F, Saxena A, Tang D, de Hoon M, Anelli V, Mione M, Carninci P, d'Adda di Fagagna F (2012) Site-specific DICER and DROSHA RNA products control the DNA-damage response. *Nature* 488: 231 – 235
9. Wei W, Ba Z, Gao M, Wu Y, Ma Y, Amiard S, White CI, Rendtlew Danielsen JM, Yang YG, Qi Y (2012) A role for small RNAs in DNA double-strand break repair. *Cell* 149: 101 – 112
10. Gao M, Wei W, Li MM, Wu YS, Ba Z, Jin KX, Li MM, Liao YQ, Adhikari S, Chong Z *et al* (2014) Ago2 facilitates Rad51 recruitment and DNA double-strand break repair by homologous recombination. *Cell Res* 24: 532 – 541
11. Pefanis E, Wang J, Rothschild G, Lim J, Chao J, Rabadan R, Economides AN, Basu U (2014) Noncoding RNA transcription targets AID to divergently transcribed loci in B cells. *Nature* 514: 389 – 393
12. Nagarajan VK, Jones CI, Newbury SF, Green PJ (2013) XRN 5′→3′ exoribonucleases: structure, mechanisms and functions. *Biochim Biophys Acta* 1829: 590 – 603
13. Houseley J, LaCava J, Tollervey D (2006) RNA-quality control by the exosome. *Nat Rev Mol Cell Biol* 7: 529 – 539
14. Luna R, Jimeno S, Marín M, Huertas P, García-Rubio M, Aguilera A (2005) Interdependence between transcription and mRNP processing and export, and its impact on genetic stability. *Mol Cell* 18: 711 – 722
15. Gavaldá S, Gallardo M, Luna R, Aguilera A (2013) R-loop mediated transcription-associated recombination in *trf4*Δ mutants reveals new links between RNA surveillance and genome integrity. *PLoS ONE* 8: e65541
16. Wahba L, Gore SK, Koshland D (2013) The homologous recombination machinery modulates the formation of RNA-DNA hybrids and associated chromosome instability. *Elife* 2: e00505
17. Sadoff BU, Heath-Pagliuso S, Castaño IB, Zhu Y, Kieff FS, Christman MF (1995) Isolation of mutants of *Saccharomyces cerevisiae* requiring DNA topoisomerase I. *Genetics* 141: 465 – 479

18. Tishkoff DX, Rockmill B, Roeder GS, Kolodner RD (1995) The *sep1* mutant of *Saccharomyces cerevisiae* arrests in pachytene and is deficient in meiotic recombination. *Genetics* 139: 495 – 509
19. Lee SE, Moore JK, Holmes A, Umezu K, Kolodner RD, Haber JE (1998) *Saccharomyces* Ku70, Mre11/Rad50 and RPA proteins regulate adaptation to G2/M arrest after DNA damage. *Cell* 94: 399 – 409
20. Page AM, Davis K, Molineux C, Kolodner RD, Johnson AW (1998) Mutational analysis of exoribonuclease I from *Saccharomyces cerevisiae*. *Nucleic Acids Res* 26: 3707 – 3716
21. Burkard KT, Butler JS (2000) A nuclear 3′–5′ exonuclease involved in mRNA degradation interacts with Poly(A) polymerase and the hnRNA protein Npl3p. *Mol Cell Biol* 20: 604 – 616
22. Mantiero D, Clerici M, Lucchini G, Longhese MP (2007) Dual role for *Saccharomyces cerevisiae* Tel1 in the checkpoint response to double-strand breaks. *EMBO Rep* 8: 380 – 387
23. Johnson AW (1997) Rat1p and Xrn1p are functionally interchangeable exoribonucleases that are restricted to and required in the nucleus and cytoplasm, respectively. *Mol Cell Biol* 17: 6122 – 6130
24. Ira G, Pellicioli A, Balijja A, Wang X, Fiorani S, Carotenuto W, Liberi G, Bressan D, Wan L, Hollingsworth NM *et al* (2004) DNA end resection, homologous recombination and DNA damage checkpoint activation require CDK1. *Nature* 431: 1011 – 1017
25. Shim EY, Chung WH, Nicolette ML, Zhang Y, Davis M, Zhu Z, Paull TT, Ira G, Lee SE (2010) *Saccharomyces cerevisiae* Mre11/Rad50/Xrs2 and Ku proteins regulate association of Exo1 and Dna2 with DNA breaks. *EMBO J* 29: 3370 – 3380
26. Chen H, Lisby M, Symington LS (2013) RPA coordinates DNA end resection and prevents formation of DNA hairpins. *Mol Cell* 50: 589 – 600
27. Saponaro M, Callahan D, Zheng X, Krejci L, Haber JE, Klein HL, Liberi G (2010) Cdk1 targets Srs2 to complete synthesis-dependent strand annealing and to promote recombinational repair. *PLoS Genet* 6: e1000858
28. van Dijk EL, Chen CL, d'Aubenton-Carafa Y, Gourvennec S, Kwapisz M, Roche V, Bertrand C, Silvain M, Legoix-Né P, Loeillet S *et al* (2011) XUTs are a class of Xrn1-sensitive antisense regulatory non-coding RNA in yeast. *Nature* 475: 114 – 117
29. Kim JA, Haber JE (2009) Chromatin assembly factors Asf1 and CAF-1 have overlapping roles in deactivating the DNA damage checkpoint when DNA repair is complete. *Proc Natl Acad Sci USA* 106: 1151 – 1156
30. Fanning E, Klimovich V, Nager AR (2006) A dynamic model for replication protein A (RPA) function in DNA processing pathways. *Nucleic Acids Res* 34: 4126 – 4137